Chiral interactions of histidine in a hydrated vermiculite clay†

Donald G. Fraser,*[a] H. Christopher Greenwell,[b] Neal T. Skipper,[c] Martin V. Smalley,[d] Michael A. Wilkinson,[ce] Bruno Demé[e] and R. K. Heenan[f]

Received 1st August 2010, Accepted 12th October 2010
DOI: 10.1039/c0cp01387k

Recent work shows a correlation between chiral asymmetry in non-terrestrial amino acids extracted from the Murchison meteorite and the presence of hydrous mineral phases in the meteorite [D. P. Glavin and J. P. Dworkin, *Proc. Natl. Acad. Sci. U. S. A.*, 2009, **106**, 5487–5492]. This highlights the need for sensitive experimental tests of the interactions of amino acids with clay minerals together with high level computational work. We present here the results of *in situ* neutron scattering experiments designed to follow amino acid adsorption on an exchanged, 1-dimensionally ordered *n*-propyl ammonium vermiculite clay. The vermiculite gel has a (001) *d*-spacing of order 5 nm at the temperature and concentration of the experiments and the *d*-spacing responds sensitively to changes in concentration, temperature and electronic environment. The data show that isothermal addition of D-histidine or L-histidine solutions of the same concentration leads to an anti-osmotic swelling, and shifts in the *d*-spacing that are different for each enantiomer. This chiral specificity, measured *in situ*, in real time in the neutron beam, is of interest for the question of whether clays could have played an important role in the origin of biohomochirality.

Introduction

Understanding the interaction of biomolecules such as amino acids and simple sugars with hydrated mineral surfaces is key to unraveling the origins of life on Earth.[2] The chirality of some crystalline mineral phases, such as quartz and calcite, has long been proposed as a possible mechanism for selectively determining the production of particular prebiotic enantiomers.[3] However, neither calcite nor quartz has been shown to have any heterogeneous catalytic function in aiding biomolecule polymerization. Fundamental questions arise as to how the first organic molecules arrived on Earth and were built up into complex molecules through prebiotic chemistry, whilst being protected from the harsh environment present at that time. Though the view that life arose *via* an "RNA World" scenario is widely supported,[4,5] there is also an alternative hypothesis that proteins originated first on the early Earth.[6] Lambert has recently reviewed the organization and polymerization of amino acids at mineral surfaces.[7]

Clay minerals have been shown to be efficient at concentrating amino acids from solution[8–10] and especially those with charged side groups, such as lysine or histidine. Clays have also been shown to catalyze peptide bond formation in their own right[11–13] and when used in conjunction with salt induced peptide formation (SIPF) chemistries.[14–16]

In carbonaceous chondrite meteorites, clay minerals are also present and have been shown to be of potential importance in protecting organic molecules from oxidizing conditions.[17] At least 70 chiral amino acids have been identified in meteorites. These were initially believed to show almost no chiral selectivity, being close to 50 : 50 racemic mixtures,[18] but recently an important and significantly greater chiral asymmetry in isovaline extracted from the Murchison meteorite has been reported[1] and this cannot have been the result of terrestrial contamination. Laboratory gas condensation experiments also generate amino acids, though again, these show almost no chiral selectivity.[19] In contrast, amino acids in proteins and enzymes in organisms are usually 100% L-enantio-specific.

Prebiotic chemistry must address the question of homochirality and the emergence of only L-amino acids in virtually all living organisms. It is known that, once seeded with one enantiomer, clay surfaces enhance selectivity for that enantiomer during crystallization cycles[20] and recent experiments have pointed towards chirally selective adsorption and reactivity in clay mineral suspensions.[21,22] Anionic clays have also been shown to have kinetic chiral selectivity for histidine.[23] The anionic clays have much higher charge density and packing than for the cationic systems. Yu *et al.* used density functional theory computer simulations to examine the energy of L- and D-alanine on the surface of nontronite clay, finding a preference by some 25 kJ mol^{-1} for the L-form.[23] Adsorption of amino acids at clay mineral surfaces is also of interest in a range of natural phenomena.[24–26] Industrially, amino acid chiral selectivity and racemization stabilization effects have been observed in anionic clays (layered double hydroxides).[27]

[a] *Department of Earth Sciences, University of Oxford, Parks Road, Oxford OX1 3PR, UK. E-mail: don@earth.ox.ac.uk*
[b] *Department of Chemistry, Durham University, South Road, Durham DH1 3LE, UK*
[c] *Department of Physics & Astronomy, University College London, Gower Street, London WC1E 6BT, UK*
[d] *Department of Physics, University of York, Heslington, York YO10 5DD, UK*
[e] *Institut Laue Langevin, F-38042 Grenoble, Cedex 9, France*
[f] *ISIS Facility, Rutherford Appleton Lab, HSIC, R3 1-22, Didcot, OX11 0QX, UK*

† Electronic supplementary information (ESI) available: Certificates of purity of amino acid reagents used. See DOI: 10.1039/c0cp01387k

In many adsorption studies, structural analysis of the clay–amino acid system is often conducted post reaction, whereas there are no high-resolution *in situ* structural studies of fully hydrated systems. In the work presented here, we studied the addition of D- and L-histidine to *n*-propylammonium vermiculite gels (with layer spacing ~50 Å). The alkylammonium vermiculite gels have been established as a model system for studying clay swelling and colloid stability.[28] The swelling is nearly perfectly one-dimensional, taking place perpendicular to the plane of the silicate layers, and leads to the formation of gels with *d*-values between 40 and 900 Å along the swelling axis. Even for the largest expansions, this *d*-value remains sufficiently well defined to be measured by small-angle neutron diffraction (SANS).

Experimental

Crystals of natural Eucatex vermiculite of dry composition $Si_{6.13}Mg_{5.44}Al_{1.65}Fe_{0.50}Ti_{0.13}Ca_{0.13}Cr_{0.01}K_{0.01}O_{20}(OH)_4Na_{1.29}$ were exchanged in NaCl and $CH_3CH_2CH_2NH_2{\cdot}HCl$ (Sigma-Aldrich 242 543, >99%) solutions over a period of several years. Around two weeks before the experiments, crystals of approximate dimensions 10 × 10 × 2 mm were placed in stock solution of propylammonium chloride in D_2O at the required concentration, and were equilibrated for the neutron scattering experiments with regular exchange of supernatant solution. Matched solutions containing D-histidine (Puriss® 53 321, ≥ 99%) or L-histidine (ReagentPlus® H8000, ≥ 99%) were made by addition of reagent to D_2O or identical stock solution of propylammonium chloride. Both amino acids were analysed and certificated by thin layer chromatography and certificates of purity are given in the ESI.†

Individual equilibrated gel crystals were selected from solution and placed in sample containers. The samples were then bathed in solution as detailed below. The swollen gels are extremely soft and delicate, and all handling was conducted under solution.

Preliminary experiments were conducted on the LOQ instrument at the ISIS Pulsed Neutron source, Rutherford Appleton Laboratory. We equilibrated stocks of gels in 0.1 M, 0.2 M and 0.35 M propylammonium chloride in D_2O. At these concentrations the *d*-spacings are approximately 110, 75 and 50 Å, respectively. As far as possible gels were selected from the stock as matched pairs, and when both showed a clear (001) Bragg peak we then exposed one to L- and one to D-histidine. In this way we studied 6 pairs in total; 1 at 0.1 M, 2 at 0.2 M and 3 at 0.36 M.

Samples were placed flat on the bottom of sealed 10 × 10 mm Hellma QS cells and were bathed in 3 cm^3 of the supernatant solution of the required concentration. The sample height and alignment was adjusted individually by laser beam, and the small angle neutron scattering was measured in the *Q* range 0.006–0.24 $Å^{-1}$. After this initial characterisation the samples were exposed to amino acid by the addition of 0.5 cm^3 of 0.18 m L- or D-histidine in D_2O. After approximately 1 hour the neutron scattering was measured again. Temperature was maintained at 30 ± 1 °C throughout by a water bath in thermal contact with the sample block.

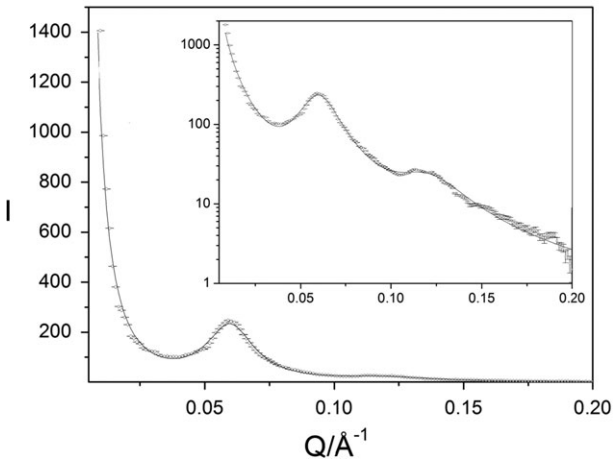

Fig. 1 Example of neutron scattering intensity *I* (arbitrary units) obtained from the instrument LOQ for the sample exposed to 0.1 M propyl ammonium chloride before exposure to L-histidine. Data (+) and fit (line). Inset shows intensity *I* on a $\log_{10}$ scale.

Cycles through a temperature range were conducted to confirm the crystal–gel transition.

Scattering intensity was corrected for background from the empty container and normalised to an absolute scale by reference to a water standard and a beam transmission measurement. Because of the sample orientation, the Bragg scattering from the (00*l*) reflections was recorded in the top and bottom quadrants of the area detector. The data were binned in *Q* with a constant bin-width of 0.001 $Å^{-1}$. The scattered intensities were fitted with the program *Fish* [Heenan, R. K. *Fish data analysis program*, RAL-Report-89-129, Rutherford Appleton Laboratory (UK) 1989] using Lorentzian Bragg profiles with a form factor derived for a distribution of oriented sheets.[29,30] Example fits are shown in Fig. 1.

In all cases the *d*-spacing was increased at constant concentration by exposure to histidine. If we express this expansion in terms of the fractional change d/d_0 then the average shift is 1.117 ± 0.020 for L-histidine and 1.102 ± 0.020 for D-histidine. The average expansion was therefore 1.5% greater for L-histidine than D-histidine, but tantalisingly, this is on the limit of the statistical precision of the experiments.

Following these initial studies on the LOQ instrument at ISIS we exploited the increased *Q*-range of station D16 at the Institut Laue-Langevin, Grenoble, to measure 1st and higher order (00*l*) peaks in both the crystalline and gel phases of propylammonium ion substituted vermiculite clay. The instrument was operated at a constant wavelength of 4.728 Å with a pixelated detector giving a *Q*-range of 0.04–0.5 $Å^{-1}$ with a bin-width of 0.0025 $Å^{-1}$. The detector efficiency was normalized by reference to a water standard. Samples of gel phase propylammonium vermiculite were prepared *via* the method of Williams *et al.*,[31,32] by soaking crystals in a deuterated solution of 0.34 M propylammonium chloride. We first measured the structure of the gels in the absence of amino acid as a control. Clay gels were equilibrated in 0.3387 M propylammonium chloride in D_2O and a

Fig. 2 Vermiculite clay gel in solution for measurement on D16.

high-quality sample was cleaved into two halves (Fig. 2). Each half was then placed in a QS cell with 4 × 10 mm sample space under supernatant solution and was aligned using a laser beam and then *via* a rocking curve centred on the (001) Bragg reflection. Temperature was maintained at 25.5 ± 0.5 °C *via* a thermal bath connected to a neutron-transparent thermal jacket.

After measurement on the samples under pure 0.3387 M propylammonium chloride in D_2O, the solution was replaced with 0.3387 M propylammonium chloride containing either 0.05 m L- or D-histidine in D_2O. After 5 full exchanges of solution over the samples, conducted over a period of around 6 hours during which the neutron scattering profile was monitored, steady state equilibrium was achieved. The final profile was then measured.

The normalized intensities were fitted as before using the program *Fish* using Lorentzian Bragg profiles with a form factor derived for a distribution of oriented sheets. A typical fit is shown in Fig. 3.

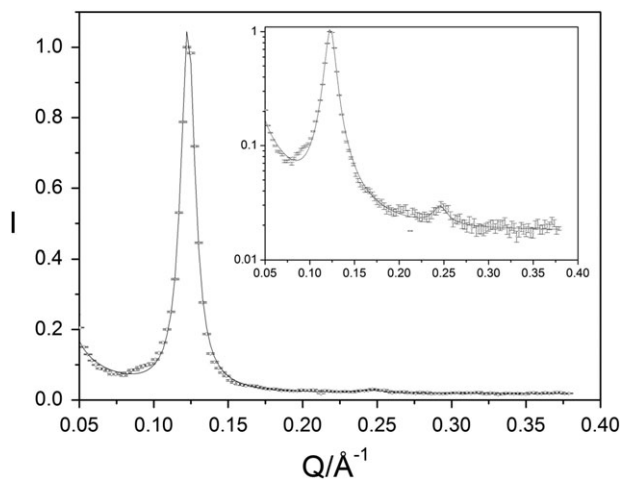

Fig. 3 Example of neutron scattering intensity I (arbitrary units) obtained from the instrument D16 for the sample exposed to 0.3387 M propyl ammonium chloride and 0.05 m L-histidine. Data (+) and fit (line). Inset shows intensity I on a $\log_{10}$ scale.

Results

It is known experimentally that for the concentrations used here, the crystal–gel phase transition for *n*-propyl-NH_3 Cl-vermiculite occurs at around 310 K.[28] This is easy to observe in the neutron beam and is completely reversible. Our hypothesis was that the thermodynamics of the phase diagram and the interlayer *d*-spacings of the clay would be sensitive to the adsorption of histidine enantiomers onto the clay surface, and that we should therefore be able detect their uptake/location and any preferential chiral interaction. Fig. 4 shows data obtained for the two nearly identical halves of untreated gel measured first in pure 0.34 M propylammonium solution. These can be compared in the same figure with the data for the same vermiculite samples measured after 5 exchanges in L- and D-histidine respectively.

The peak in all cases arises from the (001) Bragg reflection—and it therefore directly gives the *d*-spacing of the sample. An ordinary increase in solute concentration causes the *d*-spacing to contract. The data in Fig. 4 show clearly that the amino acids act "anti-osmotically" so that addition of amino acid, and hence increase in the overall solute concentration, causes the *d*-spacing to widen relative to that of the pure control clay system. This suggests that histidine adsorbs to the clay surface, screening the Coulombic charge. In addition, there is evidence of a chiral shift: L-histidine increases the *d*-spacing relative to D-histidine. The value for the control was 48.78 Å; D-histidine shifted from 49.06 to 50.33 Å; L-histidine shifted from 48.76 to 51.11 Å. Previous studies of these gels have established the relationship between *d*-spacing and concentration in propylammonium chloride solutions.[28] In the region of most interest, around 0.35 M, the equilibrium *d*-spacing increases by around 1 Å for a 0.01 M decrease in concentration. The solutions were prepared by weighing both solute and solvent on a four decimal point chemical balance. The changes we report here are therefore easily significant when compared with the reliability of the solution concentrations. The ~1.5% difference between L- and D- is significant in terms of the accuracy of the instrument and is also consistent with our previous experiments on LOQ.

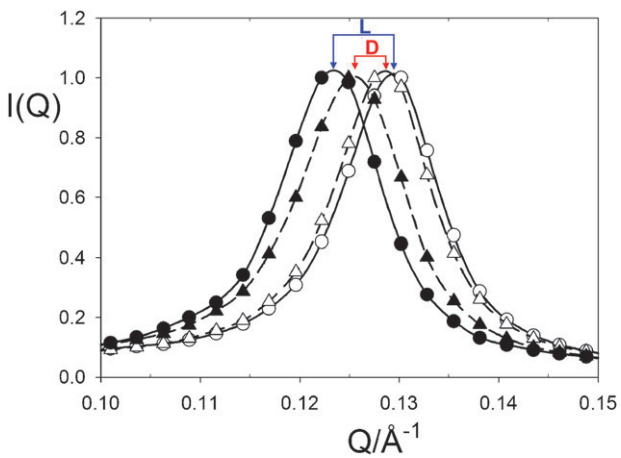

Fig. 4 Shift in *d*-spacing of histidine intercalated propyl-ammonium vermiculite clay gels and control systems. L-histidine and control: filled and empty circles. D-histidine and control: filled and empty triangles.

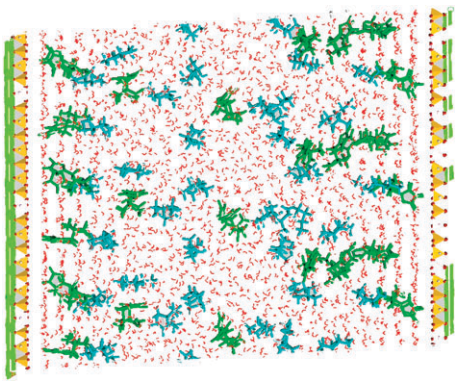

Fig. 5 Schematic based on molecular simulations showing interlayer arrangement of histidine (green coloured) molecules in a propylammonium (blue molecules) vermiculite clay (color: Si = orange; Al = magenta; Mg = green; O = red; H = white).

To provide further information on the nature of the amino acid adsorption, a separate experiment was conducted in which a previously L-histidine-equilibrated sample was exposed to D-histidine. In this case there was no significant reverse shift in the *d*-spacing on going from L- to D-over the timescale of the experiment (~6 hours). This lack of short term reversibility lends support to the notion that the amino acids are bound directly and strongly to the clay surface. The conclusion that amino acids, once adsorbed on the vermiculite gel interlayer, are quite strongly bound and difficult to displace is supported independently by DFT simulations.[23]

To aid visualization, a molecular graphics snapshot of the interlayer region of the hydrated clay is shown in Fig. 5. A super cell was generated using the methodology of Skipper *et al.*[33] The super cell had dimensions of 21.12 × 18.28 × 45.55 Å. This was equilibrated using the Monte Carlo MC programme Monte, in the NVT (constant number of particles, volume and temperature) ensemble to give a hydrated propylammonium vermiculite (470 water molecules and 12 propylammonium molecules) with histidine in the interlayer.[34] In the MC simulation the interaction parameter set of Boek *et al.* was employed.[35] The MC end point simulation cell was used as the starting point for 40 ps of MD simulation, run using the Dreiding forcefield[5] with the charges previously assigned. The interlayer was expanded to the experimentally determined *d*-spacings and additional water molecules added as required. The Forcite code in the Accelrys Inc Materials Studio software was used for the MD simulations. This simulation process is similar to that employed previously by the authors.[36–38]

It is apparent from the snapshot taken after 40 ps MD simulation of a 3 × 2 replication of the end model, that a large proportion of the histidine molecules are indeed adsorbed at, or close to, the mineral surfaces as suggested by the experimental data. In simulations carried out using a similar method, phenylalanine is observed to lie parallel to the clay layers in a model montmorillonite.[39] In the present case, the histidine molecules are oriented substantially perpendicular to the vermiculite layers with the amino functionality towards the interlayer mid-plane, suggesting that the positively charged propylammonium species in the mid-plane of the interlayer act to orient the histidine molecules in this way.

To try to determine whether the effects described above were due to preferential uptake of one isomer over the other, chiral high performance liquid chromatography (HPLC) was undertaken. Experiments were carried out in 8 ml screwtop glass vials. A 250 ml stock solution of 0.40 mg per ml of DL histidine and 0.338 M $PrNH_3Cl$ was prepared. Raw Eucatex vermiculite, which had been stored under distilled water, was dried at 80 °C for 24 h. Sodium vermiculite was exchanged twice over 24 h with 0.388 M propylamine solution, and dried at 140 °C for 1 h. Different weights of clay were then added to a constant amount of histidine solution, so that the change in histidine concentration could be found. The raw vermiculite samples were left to equilibrate over 24 h, whilst the propylamine vermiculite equilibrated over 1.5 h.

Analysis method. A Perkin-Elmer Peltier plate HPLC with autosampler, in the Analytical Laboratory, Department of Chemistry, Durham University, was used for all analyses. A Crownpak CR(+) chiral HPLC column (D form eluted first) was used throughout. Stock 20% perchloric acid diluted to give pH 1 was used as an eluent, with the histidine underivatised. A temperature of 10 °C and a flow rate of 0.1 ml min^{-1} was found to give good separation and could be reliably maintained. An UV detector, λ 200 nm, was used. The retention times were 4.73 min and 6.27 min for the D- and L-histidine, respectively.

A set of standards was made up at the experimental concentration of 0.388 M and with the change in enantiomeric excess (ee) set at 5.00%, 1.00%, 0.50% and 0.05%. For a mixture of isomers the relative area under each peak, expressed as a percentage of the total of the two isomer peaks, indicates the enantiomeric excess. At 5% and 1% ee the steps were reasonably well resolved. The relative high values of the area measured (in $\mu V\ s^{-1}$) lead to a spread in the results at the lower ee of 0.5% and 0.05%. However, when these are converted to percentage ee, a clearer trend was defined. Even at 0.5% ee, the observed changes seem valid. In summary, it would seem that the instrument and method used were capable of discerning, within reasonable error, increments down to 0.05%, though the absolute value may be slightly different to the standard.

To investigate the effects of adsorption on the vermiculite clay varying weights of clay were added to the racemic mix of D/L histidine and the supernatant measured for preferential adsorption of amino acid. In addition to testing propylammonium exchanged clay as used in the neutron scattering experiments, the sodium clay and propylammonium solution were tested, and the sodium clay alone was tested to determine any effect the propyl ammonium clay/solution may have had.

Within the error present in the data, and allowing for the slight non-equivalence in the baseline solutions with no clay present, it is not possible to discern an ee in favour of either enantiomer. The size of the variation in the data was ±0.3% ee.

Thus, within the experimental errors of these measurements, we could find no evidence for preferential adsorption of either enantiomer.

Discussion

Previous experimental and theoretical work on swelling in clays has shown that the equilibrium inter-layer swelling

depends on a subtle balance of forces that involves the electrolyte concentration and the effective surface charge on the layers.[40–44] The influence of the surface charge on the layers is small relative to that of the bulk salt concentration, but importantly, lower surface charges increase swelling and hence increase the inter-layer *d*-spacing. This implies that the shift in *d*-spacing observed in these experiments is due to differences in the electrostatic screening effects of the two isomers at the layer–solution interface. As shown by Boek *et al.*,[35] a key to understanding these effects lies in differences in the interaction between molecules in the diffuse double layer and the clay gel surface. Neutron diffraction studies show that vermiculite layers in these *n*-alklammonium vermiculite gels are covered by exactly two layers of water molecules.[28] The alkylammonium counterions in the system are located partly in a layer from about 6 to 10 Å from the surface and partly in the diffuse double layer that constitutes the rest of the interlayer region. As shown in the visualization in Fig. 5, it is likely that histidine molecules replace some of the water molecules in the surface layer and because of the acidity of the clay layers, these molecules will exist in their protonated form, carrying a single positive charge.[45] Their presence at the interface will thus reduce the effective surface charge and theory predicts that such a reduction will in turn lead to an increase in the *d*-value *via* a reduction in the long-range electrostatic attraction.[43] Such a mechanism offers a plausible explanation for the 'anti-osmotic' effect referred to above—*i.e.* despite adding a solute to the system, the gels expand because of the electrostatic screening effects caused by histidine adsorption on the interlayer surface. The observed difference in effect of the two enantiomers implies that the expanded vermiculite gel surface and adsorbate be inherently chiral. While different amino acids will bind differently to the separated siloxane sheets of the substrate gel and perturb the electronic environment to different extents, we do not expect that the chiral anti-osmotic swelling observed in these experiments should be confined to amino acids with aromatic rings. Indeed the meteoritic evidence referred to above shows a correlation between hydration and the enantiomeric excess of the non-aromatic, non-terrestrial and non-contaminant amino acid, isovaline.[1] The assembly of chiral molecules is generally agreed to involve directional attractive interactions such as hydrogen bonding and π–π aromatic stacking. Interactions with surfaces are also particularly important in self-organization as has been observed by high resolution STM microscopy for adenine molecules on oxide surfaces[46] and the chiral modification of solid surfaces by symmetry removal through adsorption of amino acids and nucleic acid bases is well known *e.g.* ref. 47 and 48 Since it is likely in the present experiments that during adsorption, amino acid molecules replace some of the water molecules in the hydrated surface layer, the hydrophobicity of individual amino acids seems likely to be an important variable. As shown schematically in Fig. 5, the precise details of how amino acids replace water molecules near the siloxane surface layer and to what extent self-organization occurs are likely to be the keys to determining the chiral selectivity observed. Understanding these and energetic differences between conglomerates in solution and on surfaces in these expanded systems, now requires careful isotopically labelled experimental work and significant large scale computation.

Conclusions

In conclusion, we demonstrate using *in situ* experiments that the different enantiomers of the amino acid histidine interact differently with a clay surface. Adsorption of the amino acid alters the physical and structural properties of the clay system at low amino acid concentrations and over a long length-range. This extends considerably previous studies of adsorption and chiral selectivity by clays, which usually require high packing densities and low hydration states for differences to become apparent. We propose that the observed effect is caused by differences in electrostatic screening effects of the two isomers at the layer–solution interface related to adsorption of the amino acid molecule.

Acknowledgements

We are grateful to ISIS and ILL for neutron beamtime and two anonymous referees for their comments that improved the manuscript. We thank Dr A. Congreve, Department of Chemistry, Durham University, for assistance with HPLC measurements. DGF gratefully acknowledges financial support from Worcester College, Oxford.

References

1 D. P. Glavin and J. P. Dworkin, *Proc. Natl. Acad. Sci. U. S. A.*, 2009, **106**, 5487–5492.
2 D. G. Fraser, *Cell. Origin Life Extreme Habitats Astrobiol.*, 2004, **7**, 149–152.
3 R. M. Hazen, T. R. Filley and G. A. Goodfriend, *Proc. Natl. Acad. Sci. U. S. A.*, 2001, **98**, 5487–5490.
4 R. F. Gesteland, T. Cech and J. F. Atkins, *The RNA World: The Nature of Modern RNA Suggests a Prebiotic RNA World*, Cold Spring Harbor Laboratory Press, Cold Spring Harbor, NY, 2006.
5 R. F. Gesteland and J. F. Atkins, *The RNA World: The Nature of Modern RNA Suggests a Prebiotic RNA World*, Cold Spring Harbor Laboratory Press, Cold Spring Harbor, NY, 1993.
6 K. Plankensteiner, H. Reiner and B. M. Rode, *Curr. Org. Chem.*, 2005, **9**, 1107–1114.
7 J. F. Lambert, *Origins Life Evol. Biosphere*, 2008, **38**, 211–242.
8 A. Parbhakar, J. Cuadros, M. A. Sephton, W. Dubbin, B. J. Coles and D. Weiss, *Colloids Surf., A*, 2007, **307**, 142–149.
9 L. O. B. Benetoli, C. M. D. de Souza, K. L. da Silva, I. G. D. Souza, H. de Santana, A. Paesano, A. C. S. da Costa, C. T. B. V. Zaia and D. A. M. Zaia, *Origins Life Evol. Biosphere*, 2007, **37**, 479–493.
10 J. Ikhsan, B. B. Johnson, J. D. Wells and M. J. Angove, *J. Colloid Interface Sci.*, 2004, **273**, 1–5.
11 J. Bujdak, H. LeSon and B. M. Rode, *J. Inorg. Biochem.*, 1996, **63**, 119–124.
12 J. Bujdak and B. M. Rode, *J. Mol. Catal. A: Chem.*, 1999, **144**, 129–136.
13 J. Cuadros, L. Aldega, J. Vetterlein, K. Drickamer and W. Dubbin, *J. Colloid Interface Sci.*, 2009, **333**, 78–84.
14 H. Le Son, Y. Suwannachot, J. Bujdak and B. M. Rode, *Inorg. Chim. Acta*, 1998, **272**, 89–94.
15 B. M. Rode, H. L. Son, Y. Suwannachot and J. Bujdak, *Origins Life Evol. Biosphere*, 1999, **29**, 273–286.
16 F. Li, D. Fitz, D. G. Fraser and B. M. Rode, *Amino Acids*, 2010, **38**, 287–294.
17 L. A. J. Garvie and P. R. Buseck, *Meteorit. Planet. Sci.*, 2007, **42**, 2111–2117.
18 O. Botta, D. P. Glavin, G. Kminek and J. L. Bada, *Origins Life Evol. Biosphere*, 2002, **32**, 143–163.

19 G. M. M. Caro, U. J. Meierhenrich, W. A. Schutte, B. Barbier, A. A. Segovia, H. Rosenbauer, W. H. P. Thiemann, A. Brack and J. M. Greenberg, *Nature*, 2002, **416**, 403–406.
20 S. I. Goldberg, *Origins Life Evol. Biosphere*, 2007, **37**, 55–60.
21 B. Siffert and A. Naidja, *Clay Miner.*, 1992, **27**, 109–118.
22 T. Ikeda, H. Amoh and T. Yasunaga, *J. Am. Chem. Soc.*, 1984, **106**, 5772–5775.
23 C. H. Yu, S. Q. Newton, D. M. Miller, B. J. Teppen and L. Schafer, *Struct. Chem.*, 2001, **12**, 393–398.
24 X. C. Wang and C. Lee, *Mar. Chem.*, 1993, **44**, 1–23.
25 N. Lahajnar, M. G. Wiesner and B. Gaye, *Deep-Sea Res., Part I*, 2007, **54**, 2120–2144.
26 J. I. Hedges and P. E. Hare, *Geochim. Cosmochim. Acta*, 1987, **51**, 255–259.
27 M. Wei, Q. Yuan, D. G. Evans, Z. Q. Wang and X. Duan, *J. Mater. Chem.*, 2005, **15**, 1197–1203.
28 M. Smalley, *Clay swelling and colloid stability*, CRC/Taylor & Francis, Boca Raton, Fla, London, 2006.
29 N. T. Skipper, A. K. Soper and J. D. C. McConnell, *J. Chem. Phys.*, 1991, **94**, 5751–5760.
30 M. Kotlarchyk and S. M. Ritzau, *J. Appl. Crystallogr.*, 1991, **24**, 753–758.
31 G. D. Williams, N. T. Skipper and M. V. Smalley, *Phys. B*, 1997, **234**, 375–376.
32 G. D. Williams, A. K. Soper, N. T. Skipper and M. V. Smalley, *J. Phys. Chem. B*, 1998, **102**, 8945–8949.
33 R. J. F. L. de Carvalho and N. T. Skipper, *J. Chem. Phys.*, 2001, **114**, 3727–3733.
34 N. T. Skipper, G. Sposito and F. R. C. Chang, *Clays Clay Miner.*, 1995, **43**, 294–303.
35 E. S. Boek, P. V. Coveney and N. T. Skipper, *J. Am. Chem. Soc.*, 1995, **117**, 12608–12617.
36 N. T. Skipper, F. R. C. Chang and G. Sposito, *Clays Clay Miner.*, 1995, **43**, 285–293.
37 H. C. Greenwell, W. Jones, S. P. Newman and P. V. Coveney, *J. Mol. Struct.*, 2003, **647**, 75–83.
38 H. C. Greenwell, A. A. Bowden, B. Q. Chen, P. Boulet, J. R. G. Evans, P. V. Coveney and A. Whiting, *J. Mater. Chem.*, 2006, **16**, 1082–1094.
39 S. P. Newman, T. Di Cristina, P. V. Coveney and W. Jones, *Langmuir*, 2002, **18**, 2933–2939.
40 I. S. Sogami, T. Shinohara and M. V. Smalley, *Mol. Phys.*, 1991, **74**, 599–612.
41 I. S. Sogami, T. Shinohara and M. V. Smalley, *Mol. Phys.*, 1992, **76**, 1–19.
42 T. Shinohara, M. V. Smalley and I. S. Sogami, *Mol. Phys.*, 2003, **101**, 1883–1900.
43 I. S. Sogami, M. V. Smalley and T. Shinohara, *Prog. Theor. Phys.*, 2005, **113**, 235–250.
44 T. Shinohara, M. V. Smalley and I. S. Sogami, *Int. J. Mod. Phys. B*, 2005, **19**, 3217–3241.
45 S. Yariv, *Int. Rev. Phys. Chem.*, 1992, **11**, 345–375.
46 D. G. Fraser, D. S. Deak, S. S. Liu and M. R. Castell, *Faraday Discuss.*, 2006, **133**, 303–309.
47 Q. Chen and N. V. Richardson, *Nat. Mater.*, 2003, **2**, 324–328.
48 K. H. Ernst, *Origins Life Evol. Biosphere*, 2010, **40**, 41–50.